Mechanisms of burst release from pH-responsive polymeric microparticles.

Article

Accepted Version

Mechanisms of burst release from pH-responsive polymeric microparticles.

Khalida Rizi [a], Rebecca J. Green [a], Olga Khutoryanskaya[a], Michael Donaldson[b], Adrian C. Williams [a,*]

[a] Reading School of Pharmacy, University of Reading, Whiteknights, P.O. Box 226, Reading RG6 6AP, UK

[b] Stiefel Laboratories, Eurasia Headquarters, Concorde Road, Maidenhead, SL6 4BY, UK

[*]Corresponding author. Tel: +44 0 118 378 6196; Fax: +44 0 118 378 6562.E-mail: a.c.williams@reading.ac.uk

Abstract

Microencapsulation of drugs into preformed polymers is commonly achieved through solvent evaporation techniques or spray drying. We compared these encapsulation methods in terms of controlled drug release properties of the prepared microparticles and investigated the underlying mechanisms responsible for the "burst release" effect. Using two different pH-responsive polymers with a dissolution threshold of pH 6 (Eudragit L100 and AQOAT AS-MG), hydrocortisone, a model hydrophobic drug, was incorporated into microparticles below and above its solubility within the polymer matrix. Although, spray drying is an attractive approach due to rapid particle production and relatively low solvent waste, the oil-in-oil microencapsulation method is superior in terms of controlled drug release properties from the microparticles. Slow solvent evaporation during the oil-in-oil emulsification process allows adequate time for drug and polymer redistribution in the microparticles and reduces uncontrolled drug burst release. Electron microscopy showed that this slower manufacturing procedure generated non-porous particles whereas thermal analysis and X-ray diffractometry showed that drug loading above the solubility limit of the drug in the polymer generated excess crystalline drug on the surface of the particles. Raman spectral mapping illustrated that drug was homogeneously distributed as a solid solution in the particles when loaded below saturation in the polymer with consequently minimal burst release.

Key words: Oil in water, oil in oil, microencapsulation, spray drying, Eudragit L100, burst release, hydrocortisone.

1 Introduction

Polymeric microparticles are increasingly used for controlled drug delivery. Preparation of these microparticles from pre-formed polymers is based on modifications of three basic methods; solvent extraction/evaporation, phase separation (coacervation) and spray-drying [1]. The emulsification solvent evaporation approach is a simple and widely applied technique, extensively studied for the preparation of polylactic acid (PLA) and poly(lactic-co-glycolic) acid (PLGA) microparticles [2,3]. However, this technique uses relatively large amounts of solvents and results in a suspension of microparticles in the external phase [4-6]. To acquire a dry powder further processing, such as filtration or lyophilisation, is needed. Another frequent problem encountered using conventional emulsification methods is drug crystallisation in the external continuous phase [6]. This problem was overcome in the case of progesterone-loaded polylactide microspheres using a spray drying method, hot air being the external phase [7].

With regards to controlled-release properties, one of the difficulties often reported for polymeric microparticles is an initial high drug release from the polymer matrix, known as a "burst release effect" [5, 8-13]. In an attempt to explain this phenomenon, a number of theories have been suggested. Wang et al. (2002) related drug release to the density of the produced microparticles suggesting that denser particles result in lower release rates [11]. Other authors attributed the burst release to high residual solvent, reduced glass transition temperature, surface drug enrichment or insufficient encapsulation [13-16]. In fact, it is well established that the distribution of drugs in delivery systems influences the release characteristics [15]. However, this is often hard to quantify *in-situ* and detailed investigations into the mechanisms responsible for the burst release effect in various microencapsulation methods have not been reported.

This work evaluates microencapsulation methods in terms of optimal controlled-release characteristics and uses various analytical techniques to investigate the possible underlying mechanisms causing burst- or controlled-release properties. Two different pH-responsive polymers with a dissolution threshold of pH 6 (Eudragit L100 and AQOAT AS-MG) were used to encapsulate hydrocortisone, a model hydrophobic drug, into microparticles below and above its solubility within the polymer matrix. Varying the drug loading above and below the solubility within the polymer tests whether drug encapsulation using spray drying is only marginally dependent on the drug's affinities to the solvent and polymer used [7]. Raman microscopy was then used to investigate the spatial distribution of the drug within the produced microparticles which was related to experimental release profiles. Unlike previous studies which develop pH-responsive microparticles intended for gastro-intestinal drug delivery, the goal of this work was to develop controlled delivery

systems which respond to more subtle pH changes, such as those observed in healthy (pH 5.0-5.5) versus atopic dermatitis skin (6.0-7.0) [17, 18].

2 Materials and methods

2.1 Materials

Hydrocortisone was purchased from Sigma-Aldrich (UK). Eudragit L100 was kindly provided by Röhm (Germany). Hypromellose acetate succinate (HPMCAS) (AQOAT® AS-MG) was obtained from Shin-Etsu (Tokyo, Japan). Ethanol, dichloromethane (DCM), hexane (laboratory grades) and sorbitan sesquioleate were obtained from Sigma-Aldrich (UK). Sodium dodecyl sulphate and Liquid Paraffin BP were purchased from Fisher Scientific (UK). Sodium phosphate dibasic heptahydrate and sodium phosphate monobasic dehydrate (Sigma-Aldrich, UK) were used in the preparation of the dissolution media.

2.2 Production of pH-responsive microparticles

2.2.1 Spray drying

Microparticles were produced using a Mini Spray Dryer, Model 290 (Buchi UK Ltd) under constant operating conditions for different microparticles. The 50:50 w/w ethanol/water polymeric solutions, with or without the drug, were fed into the machine by a peristaltic pump at 1.5 ml/min (feed rate 5%) and sprayed through a 0.7mm two-fluid nozzle into the drying chamber. The flow of compressed nitrogen used to atomise the feed solution was 350 L/min. Inlet temperature was set at 70° C with a corresponding outlet temperature of ~35° C. A flow of heated nitrogen, at 28 m^3/hr (aspirator rate 75%), induced rapid evaporation of solvent from the droplets and led to the formation of solid microparticles which were collected in a high performance cyclone. In all cases the concentration of the polymer in the feed solution was maintained at 2% w/w (to circumvent changes that can arise from differences in feed solution viscosity) while varying hydrocortisone loading at 2.5, 10 and 25% w/w with respect to polymer.

2.2.2 Solvent-evaporation method

Two variations of the solvent evaporation method were investigated in this study using different external phases, either water (oil in water emulsification) or liquid paraffin (oil in oil emulsification). For the oil in water microencapsulation method, 10% w/v polymeric organic solutions were prepared by dissolving the polymer in a mixed solvent of DCM/ ethanol (7:3 v/v). This solution (10 ml) was added to 100 ml of 0.25% w/v hydroxypropyl methylcellulose (HPMC) aqueous phase. Similarly, with the oil in oil method, 15 ml of 10% w/v polymer ethanolic solution (oil_1) was

emulsified into 100 ml liquid paraffin (oil_2) containing 1% w/w of sorbitan sesquioleate as an emulsifying agent [19].

For both techniques, the emulsion was obtained by stirring (4 cm four-blade propeller) at 1200 rpm (IKA® Laboratechnik). Solvent removal was achieved by continuous stirring of the emulsion droplets at 1200 rpm overnight at room temperature to allow solvent evaporation. The solidified microparticles were then recovered by vacuum filtration (through Whatman filter paper, 0.45 µm pore size), washed with 200 ml of water in the case of the oil-in-water emulsification or with three portions of 25ml *n*-hexane after the oil-in-oil microencapsulation process. This was followed by vacuum drying for 6 hrs at room temperature. 2.5%, 10% and 25% w/w hydrocortisone-loaded microparticles were obtained by incorporating the appropriate drug amount to the initial polymeric solutions.

2.3 Yield and encapsulation efficiency

Microparticle yields were calculated by:

$$Yield = \frac{W_{recovered}}{W_{total}} \times 100 \qquad \textbf{Equation 1}$$

Where, W_{total} is the total solids weight used in the initial polymeric solution and $W_{recovered}$ is the weight of recovered microparticles. To calculate drug encapsulation efficiency, amounts of dry powder samples equivalent to 20 µg/ml theoretical hydrocortisone loading were dissolved in ethanol for Eudragit L100 microparticles and in pH7 phosphate buffer for AQOAT AS-MG (as this polymer is insoluble in ethanol). The amount of hydrocortisone encapsulated was determined by UV spectrophotometry (Jasco V-530 UV-VIS spectrophotometer) at 242 nm (ethanol) or 248 nm (pH 7 phosphate buffer) against calibration curves. The encapsulation efficiency (EE) was calculated as:

$$EE = \frac{M_{actual}}{M_{theoretical}} \times 100 \qquad \textbf{Equation 2}$$

Where, M_{actual} is the actual amount of the drug encapsulated and $M_{theoretical}$ is the theoretical amount encapsulated, calculated from the amount of drug added during the manufacturing process. All analyses were performed in triplicate.

2.4 Scanning electron microscopy

Scanning electron microscopy (SEM) was used to examine the shape and surface morphology of the microparticles. Powder samples were attached to double sided adhesive carbon tabs mounted on an

SEM support, coated with gold (Edwards Sputter Coater S150B) and assessed with a high vacuum scanning electron microscope (SEM) (Cambridge 360 stereoscan). The SEM instrument was operated at an accelerating voltage of 20 KeV and a working distance of about 15 mm.

2.5 Density

Bulk density (bρ) was measured by filling the dry powder into a 2 ml graduated syringe whose bottom was sealed with Parafilm™ [20, 21]. The weight and volume occupied by the powder was recorded to calculate bρ. The tap density (tρ) of the powders was then evaluated by tapping the syringe onto a level surface at a height of about 2 cm [20], until no change in volume was observed. The resultant volume was then recorded to calculate tρ. Each measurement was performed in triplicate.

2.6 Thermo-gravimetric Analysis (TGA)

Thermo-gravimetric analysis assessed the residual solvent within the prepared microparticles. These investigations were performed in a Q50 TA instrument (TA Instruments Ltd, UK) equipped with TA universal analysis software. Samples of about 10 mg were heated from 30 to 200°C at 20°C /minute under a nitrogen purge of 50 ml/min using a platinum pan.

2.7 Differential scanning calorimetry (DSC)

Thermal behaviour of polymers, drug, drug free microparticles and drug-loaded microparticles was analysed using differential scanning calorimetry (Q2000 TA instruments) equipped with TA universal analysis software. The apparatus was calibrated with indium prior to analysis. Approximately 4 mg samples were accurately weighed into standard aluminium pans, which were then crimped and heated from 30 to 150°C at 10°C/minute with a 30 min isothermal hold at 150°C to remove any excess moisture. The samples were then cooled to 30°C and heated to 250°C at 10°C /minute under a nitrogen purge of 20ml/min. All samples were tested in triplicate.

2.8 X-ray powder diffraction (XRPD) measurements

X-ray powder diffraction patterns of the starting materials (hydrocortisone and Eudragit L100) and microparticles were obtained using a Bruker D8 Advance diffractometer (Bruker, Germany), using Cu Kα radiation (λ= 1.5406 Å). Samples were scanned from 5 to 45° 2ϑ, with a step size of 0.017° and a count time of 3 seconds per step. Samples were rotated at 30 rpm during analyses. The generator was set to 40 keV and 40 mA.

2.9 Raman microscopy

Raman spectra were recorded using a dispersive Renishaw inVia Raman microscope coupled with a 532 nm diode laser source and a Leica DM2500 M microscope. A 100 x working-length objective was

used for optical imaging and spectral acquisition. The collected radiation was directed through a notch filter that removes the Rayleigh photons, then through a confocal hole and the entrance slit onto a grating monochromator (2400 groove/mm) that disperses the light before it reaches the charge-coupled device (CCD) detector. The spectrograph was set to provide a spectral range of 100-2000 cm^{-1}.

Depth profiling of the oil-in-oil generated microparticles was acquired at a step of 2 µm for the 25% hydrocortisone-loaded microparticles and a step of 0.8 µm for 10% and 2.5% w/w loaded-microparticles. Spectrum acquisition times were typically 180s. Spectra were collected to a total depth of 15.20 µm, for the 2.5% and 10% w/w hydrocortisone-loaded microparticles, and 38 µm for 25% hydrocortisone-containing microparticles due to their larger particle diameters. In all cases, a total of 20 spectra were acquired starting from the microparticle's surface.

2.10 In vitro dissolution testing

pH-stepped dissolution testing of the different drug-containing microparticles was performed using USP II apparatus (paddles) (Varian VK7010 dissolution system) at 50 rpm and 32±1^{o}C (which represents normal skin temperature as the microparticles are intended for topical drug delivery). The reported aqueous solubility of hydrocortisone is 0.28 mg/ml [18, 22]. Therefore, amounts of drug-containing microparticles equivalent to 0.02 mg/ml hydrocortisone on complete dissolution were used, ensuring sink conditions ($C<0.1\ C_s$). The powders were first tested in 500 ml of 0.1M pH 5 phosphate buffer for two hours, after which the pH was increased to 7 by the addition of 100 ml 0.29M NaOH, and testing then continued for a further two hours. Samples (1 ml) were withdrawn periodically, passed through a 0.45 µm membrane filter (Millipore®) and assayed by UV spectrophotometery at 248 nm, a wavelength at which no interference from the polymers was observed.

2.11 Statistical analysis

Differences in tap density measurements and maximum drug release between Eudragit L100 microparticles obtained from the two methods (spray drying and solvent evaporation) and containing different drug-loadings were assessed using one way analysis of variance, (Genstat; version 12); in all cases $p<0.05$ denoted significance.

3 Results and discussion

Unlike the solvent evaporation technique, encapsulation using spray drying is thought to be only slightly dependent on the drug's compatibility with the solvent and polymer used [7]. In this study,

the effect of drug:polymer compatibility on hydrocortisone release from the prepared microparticles was explored by incorporating the drug at levels below and above its solubility limit within the polymer matrices. The solubility of hydrocortisone in Eudragit L100 and AQOAT AS-MG was found through microscopic examination of polymer films [23]. A high solubility of the drug in the polymer matrix is indicative of high drug-polymer compatibility [6, 23] and results in better incorporation of the drug within the prepared microparticles. Hydrocortisone was found to be more soluble (13-14% w/w) in Eudragit L100 films [24] compared to AQOAT AS-MG (9-10% w/w; Figure 1).

INSERT Figure 1

Various other parameters including the physicochemical properties of both drug and polymer need to be considered for successful encapsulation of drugs into polymeric microparticles. The model drug used, hydrocortisone, has a reported water solubility of 0.28 mg/ml [16], and we previously reported its solubility in ethanol to be 11.4±0.33 mg/ml [24]. These solubility's dictate the extent of drug diffusion to the surface of the microparticles during the preparation process and ultimately affect drug release.

3.1 Preparation of pH-responsive microparticles

3.1.1 Spray drying as a microencapsulation technique

We previously reported the potential use of spray drying to prepare pH-responsive Eudragit L100 microparticles [24]. The method was optimised in terms of drug release, taking into account the effect of different solvent systems and various polymer concentrations. Using Eudragit L100 as a pH-responsive polymer, it was found that a polymer content of 2% w/w and a solvent system of 1:1 w/w ethanol/water led to the lowest drug release at pH 5, a pH at which the polymer is not soluble. Using these optimised conditions, the effect of varying the drug loading (2.5% and 25% w/w) on the release profile was investigated [24]. Here, we also report the effect of 10% w/w hydrocortisone-loading (Table 1). AQOAT AS-MG microparticles were also generated using the same conditions to explore the methods' transferability to other polymers (Table 1). Encapsulation efficiency was high, with more that 88% of the drug incorporated in all cases. Morphological characteristics of Eudragit L100 and AQOAT AS-MG microparticles containing different hydrocortisone loadings were examined with SEM imaging as shown in Figure 2. The rough morphology of these microparticles is thought to result from polymer phase separation at the surface of the drying droplets [24].

INSERT Table 1

INSERT Figure 2

Powders prepared from AQOAT AS-MG tended to aggregate. The presence of aggregates increases the voids within the powder bed and results in relatively low tap densities compared with Eudragit L100 microparticles [24] (Table 1). Further investigation of the pH-responsiveness of these spray dried microparticles, from pH 5 to 7, demonstrated that AQOAT AS-MG particles dissolve at a lower pH than expected, between pH 5.3 and 5.4 (data not shown). Similar observations were reported by Friesen et al who found AQOAT AS-MG soluble above pH 5.2 [25]. In contrast, Eudragit L100 microparticles dissolved at pH 5.8 to 5.9, close to the reported polymer solubility threshold of pH 6 [24]. Differential scanning calorimetry did not show any changes between the polymer microparticles and the initial AQOAT AS-MG powder (data not shown). The discrepancy in pH-responsiveness between the manufacturer information and experimental results for AQOAT AS-MG might be a result of differences in testing methodologies; the manufacturer's information is based on disintegration testing of 1 cm^2 polymeric films which may dissolve more slowly than the microparticles [26].

Due to the relatively high drug burst release observed previously with spray-dried Eudragit L100 microparticles at pH 5 and 1.2 [24], pHs at which the polymer is not soluble, an alternative microencapsulation technique, namely, the solvent-evaporation method, was investigated.

3.1.2 Oil-in-water emulsification/solvent evaporation technique

In the oil in water emulsification process, the drug and polymer are first dissolved in a water-immiscible solvent, usually dichloromethane (DCM), and the resulting organic phase is emulsified into an aqueous phase containing an appropriate emulsifier. The organic solvent can then be removed by evaporation or extraction. The method has been used to prepare Eudragit-based systems, for the sustained release grades RL and RS [27, 28], which are neutral copolymers of poly (ethylacrylate, methyl methacrylate) and trimethyl aminoethyl methacrylate chloride [27]. pH-responsive particles have also been successfully prepared using Eudragit P-4135F [29-31]; Eudragit P-4135F is synthesised by the co-polymerisation of methacrylic acid, methyl methacrylate and methyl acrylate [31] and exhibits a dissolution threshold of pH 7.2 [31].

The above Eudragit grades are all soluble in DCM, which is advantageous as it facilitates the emulsification of the polymer solution. Moreover, the limited solubility of DCM in water prevents drug loss to the external aqueous phase which can occur with solvent diffusion. However, Eudragit L100 is not soluble in DCM whereas AQOAT AS-MG is only partially soluble (swellable) [32]. Therefore, a mixed solvent of 7:3 v/v DCM/ethanol was used to solubilise the polymers in the initial organic phase [33-36]; the ethanol content was minimised to limit drug diffusion into the aqueous phase.

Using the DCM/ethanol cosolvent system, microparticles were successfully prepared using a 10% w/v AQOAT AS-MG organic solution (Figure 3). The hollow nature of these microparticles is attributed to rapid ethanol diffusion followed by polymer precipitation [35]. The rate of solvent diffusion during the initial stage of microparticle preparation is determined by its water solubility. The aqueous solubility of DCM at 25°C is 1.85% [2, 11] whereas ethanol is completely miscible with water. The partial solubility of AQOAT AS-MG in DCM means that the polymer shell formed at the interface of the emulsification droplets is non-rigid. This allows for DCM evaporation through eruptions in the polymeric shell. The net result is the formation of spherical intact microparticles with a porous surface upon complete shell solidification (e.g. Figure 3, D).

INSERT Figure 3

These morphological observations are consistent with tap density measurements of AQOAT AS-MG microparticles (Table 2), which are considerably lower than those calculated for the spray dried powders (Table 1) and are attributed to the hollow nature of the particles. However, hydrocortisone encapsulation into AQOAT AS-MG microparticles resulted in relatively low encapsulation efficiencies (Table 2) probably as a result of rapid ethanol flux into the external aqueous phase. A comparable phenomenon was reported in the literature for the encapsulation of estradiol and indometacin into Eudragit L100-55 [6].

INSERT Table 2

Although hydrocortisone is a hydrophobic drug, it exhibits an appreciable solubility in aqueous media of 0.28 mg/ml [16]. The diffusion of ethanol into the external aqueous phase during the emulsification process leads to drug leaching and increased hydrocortisone solubility in the external aqueous phase. This phenomenon may explain the low encapsulation efficiency measured and the appearance of drug crystals in the external aqueous phase at 25% w/w theoretical drug loading (Figure 3, C). Microparticles prepared at 2.5% w/w drug loading show similar morphological characteristics to the drug-free microparticles with no visual evidence of drug crystallisation (Figure 3, B). Nonetheless, the encapsulation efficiency of the drug was low despite the fact that it was incorporated at a level well below its solubility limit within the polymer.

In contrast, at 10% w/w polymer concentration, sticky Eudragit L100 droplets were produced during the early stages of the oil-in-water emulsification process leading to the formation of elongated polymeric structures (data not shown). In an attempt to overcome this problem, a reduced polymer concentration was used to decrease polymer-polymer interactions in the initial polymeric organic solution which, in turn, reduces the polymer's tendency for precipitation and enables polymer

emulsification into the external aqueous phase. Nonetheless, the emulsified droplets generated in the early stages of particle formation tended to collapse during the solvent evaporation step (Figure 3, E), possibly due to the brittle nature of the Eudragit L100 shell that forms at the interface of the droplets. The glass transition temperature of Eudragit L100 was reported to be about 160^{o}C with a corresponding minimum film formation temperature (MFT) of 85^{o}C [36]. Similarly to AQOAT AS-MG, the hollow nature of Eudragit L100 microparticles is attributed to rapid ethanol diffusion, polymer precipitation and subsequent shell formation.

3.2 Oil-in-oil emulsification/solvent evaporation technique

An oil-in-oil emulsification process was adopted to circumvent the problem of drug leakage into the external phase. Kendall et al have recently developed a reproducible oil-in-oil microencapsulation method for fabricating Eudragit L100 microparticles intended for gastrointestinal delivery [19]. The method uses liquid paraffin, a non-solvent for both drug and polymer, as the external oil phase. Despite the fact that the use of DCM (ICH class 2) was avoided and ethanol (ICH class 1) was chosen to solubilise the polymer in the internal oil phase, the utilisation of hexane (ICH class 2) for external oil phase removal is inevitable.

Drug-free Eudragit L100 microparticles prepared from a 10 % w/v polymeric solution using the oil-in-oil emulsification process have a smooth surface and are less polydisperse than microparticles produced from the spray drying method (Figure 4) with no observed surface porosity. The solubilisation of 2.5% and 10% w/w hydrocortisone in the initial polymeric solution led to the formation of spherical microparticles with similar morphological characteristics. At 25% w/w theoretical drug loading, hydrocortisone was not fully soluble in the initial polymeric solution due to its limited solubility in ethanol. Therefore, the non-solubilised drug crystals are incorporated into relatively large microparticles (about 150 µm diameter compared with 30 µm diameter for drug-free, 2.5 and 10% drug-loaded microparticles) (Figure 4). The presence of drug crystals at a relatively high theoretical loading might have increased the viscosity of the initial polymeric solution. A more viscous phase will require larger shear stress (stirring in this case) to break the emulsion droplets into smaller sizes.

INSERT Figure 4

Yield, encapsulation efficiency and tap density results obtained from the emulsification of 10% w/v polymeric solutions into liquid paraffin are presented in Table 3. The encapsulation efficiencies obtained for hydrocortisone are relatively high, comparable to those calculated for the spray dried powders (Table 1). The lower encapsulation efficiency at 25% w/w theoretical drug loading can be

explained by the loss of uncoated drug crystals into the external oil phase. The high tap density measurements obtained for the oil in oil microparticles suggest that they are solid. However, the oil-in-oil generated Eudragit L100 microparticles with 25% hydrocortisone-loading presents a low tap density due to the presence of crystals within the microparticles which might have disturbed their internal structure and led to pore formation (Figure 4, D).

INSERT Table 3

The relatively high polymer concentration (10 % w/v), used in the internal oily phase, increased polymer viscosity and caused rapid droplet solidification [2]. The rapid solidification of microparticles is advantageous in achieving high drug encapsulation efficiency as it hinders drug migration to the particles' surface [2]. In fact, a 1% w/v Eudragit L100 concentration led to inefficient hydrocortisone encapsulation with apparent drug crystals in the external phase and on the surface of the dried microparticles (data not shown). In this case, the low polymer viscosity and slow droplet solidification allowed more time for drug loss through diffusion.

The transferability of the oil-in-oil microencapsulation method to different grades of Eudragit; L100, S100 and L55, has been reported by Kendal et al. [19]. Nonetheless, its applicability to structurally non-related polymers has not been investigated. Here, the oil-in-oil emulsification method was used to prepare AQOAT AS-MG microparticles but the initial oil phase was substituted by a 7:3 v/v DCM/ethanol co-solvent system to allow for AQOAT solubilisation. SEM images of the obtained microparticles show similar morphological characteristics to Eudragit L100 particles but with a rougher surface topography (Figure 4, E and F).

Unlike the oil-in-water emulsification method, the microparticles obtained from the oil-in-oil microencapsulation process appear to be solid. This can be attributed to the relatively slow "good solvent" (ethanol) removal rate. This allows time for polymer redistribution within the drying droplets and results in the formation of solid microparticles. Even when a mixed solvent of DCM/ethanol is used, as for AQOAT AS-MG, the morphology of the particles obtained is similar to that for Eudragit using ethanol alone.

3.3 Drug release

From the different microencapsulation techniques tested, spray drying and the oil-in-oil microencapsulation method resulted in the successful formation of microparticles with efficient drug encapsulation. Dissolution data of these powders are in Figure 5, showing stepped dissolution of microparticles below and above the pH solubility of the polymer. Although the size of the microparticles can influence the rate of drug release in the initial stages, here we compare total drug

release after 2 hours at pH 5, when a plateau is reached. Total drug release at this stage is more likely to be due to other factors such as particles porosity or drug distribution. In fact, a study that investigated the release 5-fluorouracil-loaded PLGA-based microparticles has showed that underlying drug release mechanisms were independent of the microparticle size [37]. Although the different size fractions released the drug at different rates initially, they all reached the same level of relative drug release after 21 days [37].

INSERT Figure 5

With both preparation methods, Eudragit L100 microparticles showed better controlled release properties than AQOAT AS-MG microparticles, i.e. lower relative drug release after 2 hours at pH 5. At 2.5% and 10% w/w hydrocortisone-loading, Eudragit L100 microparticles obtained from the oil-in-oil encapsulation technique led to negligible hydrocortisone release at pH 5 (Figure 5, B). At 25% w/w drug loading, due to the limited solubility of hydrocortisone in ethanol (11.4±0.33 mg/ml), about 50% of the drug was not dissolved in the initial polymeric solution. During the emulsification process, the non-dissolved drug crystals preferentially distribute on the particles' surface (Figure 4, D) resulting in about 40% drug burst release at pH 5 after 2 hours (Figure 5, B). This suggests that the remaining 10% of undissolved drug crystals is incorporated deeper into the polymer matrix. In contrast, regardless of the drug loading level, the spray dried powders showed a high burst release effect at pH 5, a pH at which the polymer is not soluble (Figure 5, A).

These variations in drug release can be attributed to differences in microparticle formation during manufacture. The burst release observed from the spray-dried microparticles implies that they are porous; the presence of pores within microparticles leads to rapid water penetration inside the particles and subsequent rapid diffusion of the encapsulated drug. The process of pore formation during spray drying arises from phase separation during the encapsulation process and subsequent drug partitioning between polymer-poor and rich regions within the drying droplet [24]. This phenomenon results in some drug entrapped within the polymer-poor region which dries to form pores or less supported structures [11].

Interestingly, the spray dried microparticles containing hydrocortisone below the solubility limit within the polymer (2.5 and 10% w/w) provided lower burst release than at 25% w/w loading (Figure 5, A). Spray drying below the solubility limit of the drug might lead to higher drug content in the polymer-rich regions of the dried particles and possibly better controlled release properties. Nonetheless, at 2.5% and 10% w/w hydrocortisone loading, the burst release at pH 5 was only reduced by about 10% at 2 hours compared to that when the drug exceeded its solubility at 25%

w/w load. This implies that either; a) drug partitioning to polymer-poor regions was still predominant or b) drug enrichment at the surface was also accounting for the drug burst release. As the evaporating droplet shrinks, its receding droplet surface leads to increased solute concentration at the surface and subsequent diffusional flux to the centre [38]. During the spray drying process, high solvent evaporation rates can lead to rapid droplet shrinking which does not allow time for drug redistribution and results in surface drug enrichment [14].

On the other hand, with the oil-in-oil microencapsulation process, solvent evaporation occurs more slowly as the emulsified droplets are stirred overnight at room temperature to allow for complete solvent evaporation. The relatively long evaporation time during the oil-in-oil microencapsulation process, compared with the fast solvent evaporation during spray drying, allows adequate time for both drug and polymer redistribution and diffusion to the centre of the emulsified droplets which may result in better controlled release characteristics. Moreover, the long evaporation time is less likely to produce porous microparticles. In comparison to Eudragit L100 microparticles, hydrocortisone-loaded AQOAT AS-MG particles resulted in a significantly higher drug release at pH 5 (Figure 5, C & D) despite the fact that the drug was incorporated at 2.5% w/w, a level well below the solubility limit of hydrocortisone within the polymer matrix. This can be attributed to differences in the internal phase solvent system. The use of a DCM/ethanol co-solvent system may lead to a more porous structure due to the relatively fast evaporation of DCM and might explain the lower tap density measurements obtained for AQOAT AS-MG microparticles (Table 2).

It is notable that the rate of drug release from the oil in oil microparticles at pH 7 (Figure 5, B, post 120 mins) increases with drug loading. This effect may reflect drug distribution within the polymer matrix; the more drug available at or near the surface of the particle the more rapid is the initial release since less polymer is available to hinder drug diffusion. Using the same oil in oil microencapsulation method, Nilkumhang et al. investigated partitioning of fluorescent dyes between the internal (ethanol) and external (liquid paraffin) phases and found a correlation between the partition coefficient and molecular distribution within the prepared microparticles [39]. However, in this study, the same drug is used and the partition coefficient between ethanol and liquid paraffin is therefore constant.

3.4 Mechanisms of “burst release”

3.4.1 Particle density and percentage porosity

Wang and Wang (2002) suggested that the density of the produced microparticles could profoundly influence drug release since increased particulate density can restrict the diffusion of the drug from

the microparticles [11]. Tap density measurements can offer insight into this phenomenon; assuming perfect packing of the tapped powder and a monodisperse size distribution, tap density values are approximately a 21% underestimate of particle density [40]. Although this method may not fully discriminate between subtle structural differences due to possible electrostatic interactions, especially when dealing with small particles, it has previously been useful employed to study microparticles[20] and the data supports that from our SEM imaging and Raman microscopy investigations.

Tap density measurements of the spray dried and oil-in-oil microparticles are reported in Table 1 and 3 respectively. For both polymers loaded with drug below the solubility limit (2.5% and 10% w/w), the oil-in-oil microparticles displayed significantly higher tap densities than the spray dried particles. This correlates with *in-vitro* release testing as the more dense oil-in-oil Eudragit particles showed negligible drug release at pH 5 (Figure 5, B) compared with the less dense spray dried particles of the same polymer (Figure 5, A). Likewise, the oil-in-oil generated AQOAT particles gave lower burst release at pH 5 than the equivalent spray dried material. Thus, for both polymers, significant burst release correlated with lower tap densities.

In contrast, microparticles prepared from the oil/oil method at 25% w/w drug-loading showed a significantly lower tap density measurement than other Eudragit L100 microparticles (Table 3) suggesting a higher level of intraparticulate voids ($p<0.05$). This increased porosity might be due to the presence of drug crystals in the initial polymeric solution which might have disturbed the flow of the polymer within the emulsification droplets leading to the formation of pores. Moreover, drug crystals are more likely to accumulate at the polymer/liquid paraffin interface during droplet drying and surface recession. Eudragit S100 microparticles containing 50% and 66.7% w/w prednisolone were hollow and showed an extensive amount of crystalline drug on the surface [41]. As expected, these morphological changes were also attributed to a high burst release [41]. Similarly, Yadav et al. (2009) [42] showed that increased intraparticle porosity of carbamazepine in Eudragit RSPO was due to low polymer deposition in the empty spaces between the agglomerated microcrystals. Increased drug deposition at the surface of our microparticles coupled with increased intraparticulate porosity explains the relatively high burst release of hydrocortisone from 25% w/w drug-loaded microparticles produced from the oil in oil emulsification method (Figure 5, B).

3.4.2 Residual solvent level

Burst release of rifampicin from poly(D, L-lactic acid) (PDLLA)/ Resomer (30:70) spray dried microparticles was attributed to residual solvent reducing the glass transition temperature (T_g) of the polymer, leading to accelerated water uptake and greater drug diffusion from the microparticles

[13]. The residual solvent in the microparticles prepared from the oil-in-oil and spray drying methods at different drug loadings was determined using thermo-gravimetric analysis (Table 4). No significant differences (P>0.05) were seen between the two methods of manufacture or between various drug loadings, showing that, for these particles, residual solvent effects were not responsible for burst effects. It should be noted that residual paraffin from the oil in oil method is not detected by this technique. However, paraffin is a hydrophobic non-solvent for the polymer and therefore is not expected to increase water uptake or influence drug release.

INSERT Table 4

3.4.3 Drug crystallinity

Differential scanning calorimetry and X-ray analysis of Eudragit L100, hydrocortisone, drug-free microparticles and hydrocortisone-loaded microparticles were used to identify changes in drug form that might have occurred during the encapsulation process (Figures 6 and 7). Drug encapsulation within microparticles depends on its initial state in the polymeric solution and on the preparation process [43]. Differential scanning calorimetry of untreated Eudragit L100 shows a broad phase transition between 180 and 235˚C (Figure 6). The nature of this phase transition is still unclear, but dissociation of inter-molecular hydrogen bonds and anhydride formation has been suggested [44]. The DSC curve of hydrocortisone powder show an endothermic melting peak at 222±0.7˚C (Figure 6), in accordance with the literature value of 221±2 °C [45].

INSERT Figure 6

INSERT Figure 7

Drug-free, 2.5% and 10% w/w hydrocortisone-loaded Eudragit L100 microparticles prepared from the oil-in-oil microencapsulation method did not show any additional phase transitions to those already observed in the untreated Eudragit powder. This suggests that, at 2.5% and 10% hydrocortisone loading, the drug is soluble in the Eudragit L100 polymer matrix giving rise to a solid solution. For 25% hydrocortisone-loaded microparticles, where a proportion of the drug was incorporated in its crystalline form, a small endothermic peak at around 200˚C corresponding to melting point depressed hydrocortisone crystals was observed. X-ray analysis of these samples (Figure 7) supports the DSC data with no crystalline drug found at low loadings but excess drug (at 25% w/w loading) was present in the same crystalline form as the starting material.

However, for spray dried materials, hydrocortisone-loaded Eudragit L100 microparticles show an endothermic shoulder which moves to a lower temperature as the drug loading increases (Figure 6). However, as the polymer also shows an endothermic peak in the same region, it was unclear

whether this thermal feature was due to the presence of drug crystals. From the X-ray diffraction patterns of unprocessed drug and hydrocortisone-loaded microparticles, the intense crystalline peaks at 14.5 and 17 degrees 2θ, observed for unprocessed hydrocortisone, were absent in the diffractogram of drug-containing spray dried microparticles (Figure 7). This suggests that the drug is present in an amorphous form within the spray dried microparticles. The presence of amorphous drug, coupled with the small size of spray dried microparticles may facilitate drug release and can partly explain the relatively high burst release observed for this material (Figure 5, A). However, the fact that the drug is non-crystalline at 2.5% and 10% w/w within Eudragit L100 microparticles produced from the oil-in-oil microencapsulation method suggests that this phenomenon is not solely responsible for the non-controlled burst effect; a further potential mechanism is the relatively high drug enrichment at the surface of the spray dried microparticles compared with the oil-in-oil powders.

3.4.4 Drug distribution within the microparticles

In order to clarify whether release from the microparticles relates to the spatial distribution of the drug within the polymer matrix, confocal Raman microscopy was used for depth profiling Eudragit L100 microparticles [46]. As discussed above, the evaporation of ethanol during microencapsulation can result in drug migration to the microparticle's surface resulting in surface drug enrichment which can result in a higher or more rapid drug release.

Figure 8 shows the Raman spectra of hydrocortisone and Eudragit L100 powders used for microparticle production. Hydrocortisone has characteristic Raman bands at 1643 and 1610 cm^{-1} which are consistent with C=C stretching modes at the 4-5 position [47, 48] (Figure 8). On the other hand, Eudragit L100 shows distinctive Raman peaks at 1751 and 1451 cm^{-1} which are assigned to the C=O stretching and $–CH_2-$ scissoring modes respectively [48]. The Raman spectrum of this polymer also displays relatively strong peaks at 1205, 1120, 969 and 812 cm^{-1} which are associated with C-H and C-C wagging vibrations [48].

Insert Figure 8

Raman depth profiling of Eudragit L100 microparticles at 25% w/w drug-loading is shown in Figure 9, A (data not shown for 2.5% and 10% w/w drug-loading). Based on the linear relationship between the intensity of the peak from the measured analyte and its concentration [49], the depth profiles were processed to acquire component graphs detailing the proportion of both hydrocortisone and Eudragit L100 as a function of depth (Figure 9, C, D and E). At 25% w/w drug-loading, the intensities of the characteristic hydrocortisone peaks at 1643 and 1610 cm^{-1} were variable: they increased dramatically at a depth of 12 μm then declined (Figure 9, A). This high intensity region coincides with

the presence of a drug crystal inside the microparticle as illustrated in the SEM image of a microtomed 25% w/w hydrocortisone-loaded particle where drug crystals can be seen both on the surface and within the polymer matrix (Figure 9, B). It should also be noted that this SEM image supports tap density measurements obtained for the 25% w/w drug-loaded microparticles (Table 3). The considerably lower tap density measurement of these microparticles (Table 3) compared to other powders containing lower amounts of drug is due to a higher level of intraparticulate voids. SEM images of the internal structure of 2.5% and 10% w/w hydrocortisone-containing microparticles showed no evidence of crystal inclusions.

Insert Figure 9

In the case of 2.5% and 10% w/w hydrocortisone-loading, the proportion of both hydrocortisone and Eudragit L100 remained constant throughout the depth studied (Figure 9, D and E). Assuming that these microparticles have a monodisperse size of about 30 μm (Figure 4), these results show that the concentration of hydrocortisone at the surface and the core (15.20 μm) is the same, i.e. the oil-in-oil microencapsulation process did not result in drug enrichment on the surface. In contrast, with 25% w/w hydrocortisone-loading, the proportion of hydrocortisone relative to Eudragit L100 varied depending on the presence of drug crystals within the polymer matrix (Figure 9. C). These results support SEM images and XRPD/DSC data, with regions within the particle showing increased intensities of hydrocortisone characteristic bands showing the presence of drug crystals. It should be noted that the data presented in Figure 9 is representative of three different microparticles selected randomly for each drug loading. Unfortunately, depth profiling of the spray dried microparticles for comparative purposes was not possible due to their small particle size (size range 1-5 μm, Figure 2).

Since Raman depth profiling of the oil-in-oil microparticles demonstrated that, at 2.5% and 10% w/w drug-loading, no differences in the spatial distribution of hydrocortisone existed within the polymer matrix, variations in drug release at pH 7 can be solely due to differences in the polymer/drug ratio. In other words, an increase in the proportion of Eudragit L100 relative to hydrocortisone, e.g. at 2.5% drug-loading, leads to a moderately slower drug release as a larger amount of polymer is available to hinder drug diffusion.

4 Conclusion

Of the different microencapsulation techniques tested, spray drying and the oil-in-oil emulsification method successfully formed microparticles with high levels of drug encapsulation. Scanning electron microscopy and dissolution testing revealed that the microparticles prepared from the oil-in-oil encapsulation method had more favourable morphological and release characteristics. In fact, the

encapsulation of hydrocortisone at levels below its saturation solubility within Eudragit L100; 2.5 and 10% w/w, lead to negligible release at pH 5, a pH at which the polymer is not soluble, whereas increasing the pH to 7 resulted in near instantaneous drug release. The spray dried powders, on the other hand, showed high drug burst release at pH 5. These variations in drug release are partially attributed to differences in microparticle formation. In contrast with the spray drying process, slow solvent evaporation and droplet solidification during the oil-in-oil emulsification process allows adequate time for drug and polymer redistribution which may result in denser microparticles and better controlled release characteristics. Tap density measurements showed good correlation with *in-vitro* drug release testing and SEM imaging, especially for the oil-in-oil produced microparticles, with high density particles showing better controlled release properties. Thermal, X-ray and confocal Raman analysis of the particles also demonstrates the importance of drug loading on release properties; below the solubility limit, drug was homogeneously distributed and was non-crystalline whereas exceeding the solubility generated crystalline domains in oil-in-oil generated materials with consequent burst release. Thus, both the manufacturing method (which influences particle porosity and density) and drug:polymer compatibility and loading (which affect drug form and distribution) are responsible for burst release seen from our particles.

Acknowledgements

The authors thank Stiefel laboratories Ltd, a GSK company, for their financial support through a PhD studentship which facilitated this work.

Figure legends

Figure 1. Microscopic examination of hydrocortisone/ AQOAT® AS-MG films (at 10x magnification) at; (A) 0%, (B) 9%, (C) 10% and (d) 20% w/w theoretical loading.

Figure 2. Scanning electron microscopy images of spray dried microparticles using Eudragit L100 with (A) 0% and (B) 10%, hydrocortisone loading and AQOAT-AS-MG with (C) 0% and (D) 2.5% drug loading.

Figure 3. Scanning electron microphotographs of microparticles prepared by the oil in water emulsification solvent evaporation method; (A) , (B) and (C) show AQOAT AS-MG microparticles at 0%, 2.5% and 25% hydrocortisone loading respectively. Image D and E shows 2.5% w/w hydrocortisone-loaded AQOAT microparticles at high magnification and drug-free Eudragit L100 microparticles respectively.

Figure 4. SEM photomicrographs of Eudragit L100 microparticles prepared from the oil-in-oil emulsification process at; (A) 0%, (B) 2.5%, (C) 10% and (D) 25% w/w theoretical hydrocortisone loading with respect to polymer. Images E and F show AQOAT AS-MG microparticles prepared at 0% and 2.5% hydrocortisone loading respectively.

Figure 5. Stepped dissolution testing of prepared microparticles with pH change from 5 to 7 after 2 hrs; (A) spray dried Eudragit L100 microparticles at different hydrocortisone loadings, (B) Eudragit L100 microparticles prepared using the oil-in-oil microencapsulation method, (C) 2.5% hydrocortisone-loaded AQOAT AS-MG spray dried microparticles and (D) 2.5% hydrocortisone-containing AQOAT AS-MG microparticles obtained from the oil-in-oil technique. HC denotes hydrocortisone. (mean±SD, n=3).

Figure 6. DSC thermograms of Eudragit L100 powder, hydrocortisone, drug-free and hydrocortisone-loaded Eudragit L100 microparticles produced from the spray drying and the oil in oil microencapsulation method.

Figure 7. X-ray analysis of starting materials (hydrocortisone and Eudragit L100) and hydrocortisone-loaded microparticles prepared from the oil-in-oil encapsulation method and spray drying.

Figure 8. Raman spectra of hydrocortisone (black line) and Eudragit L100 (red line).

Figure 9. Raman depth profiling (A) and scanning electron microscopy (B) showing the internal composition of 25% w/w hydrocortisone-loaded microparticles prepared from the oil-in-oil microencapsulation technique. (C), (D) and (E) represents the component analysis of hydrocortisone

(red line) and Eudragit L100 (blue line) within the oil-in-oil prepared microparticles as a function of depth. Depth profiling was performed from the surface (0 µm) to a depth of -15.2 µm for 2.5% (E) and 10% w/w (D) hydrocortisone-loaded microparticles and -38.0 µm for 25% w/w drug-containing microparticles (C). HC denotes hydrocortisone.

Table legends

Table 1. Yield, tap density and encapsulation efficiency values of Eudragit L100 and AQOAT AS-MG microparticles prepared from the spray drying method with variable hydrocortisone loadings.

Table 2. Yield and encapsulation efficiency of hydrocortisone-loaded AQOAT AS-MG microparticles prepared from the oil-in-water emulsification process.

Table 3. Yield, tap density and encapsulation efficiency values of Eudragit L100 and AQOAT AS-MG microparticles prepared from the oil in oil emulsification method at variable hydrocortisone loadings.

Table 4. Residual solvent content (% w/w) of the microparticles (MPs) prepared from the oil-in-oil and spray drying methods.

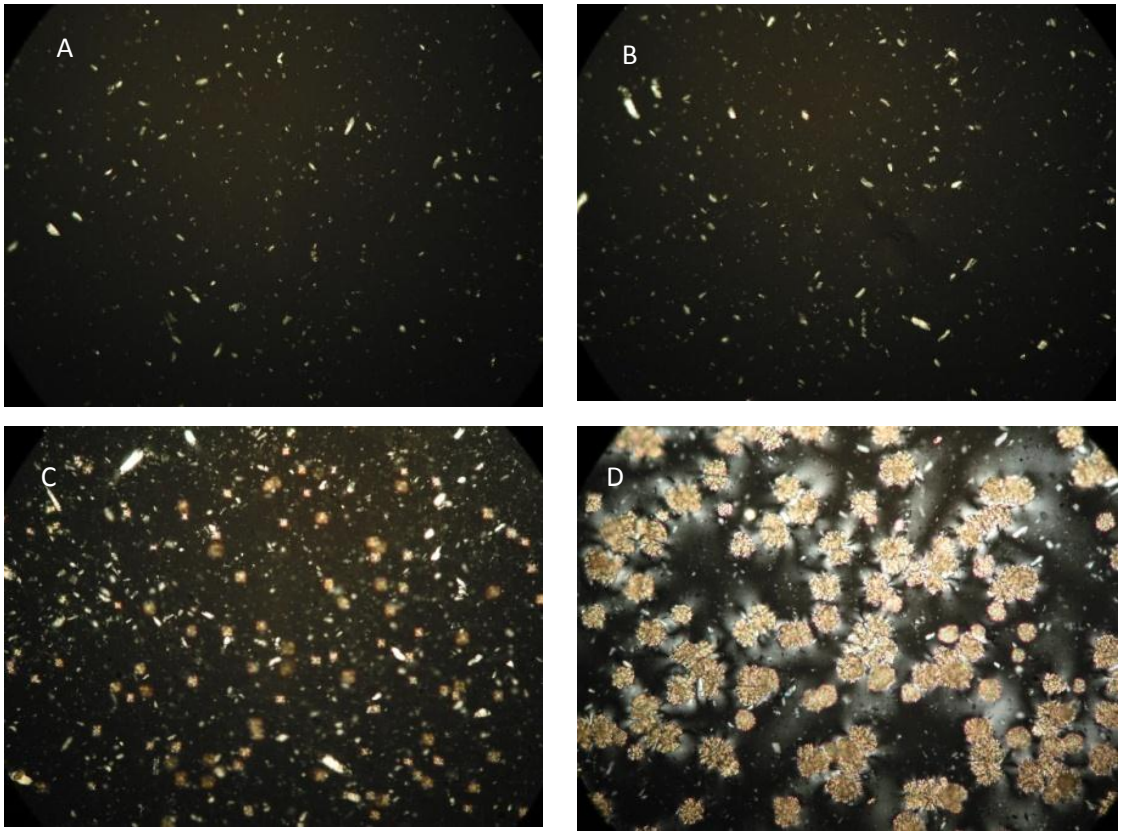

603 **Figure 1.**. ***Microscopic examination of hydrocortisone/ AQOAT® AS-MG films (at 10x magnification) at; (A) 0%, (B) 9%, (C)***
604 ***10% and (D) 20% w/w theoretical loading.***

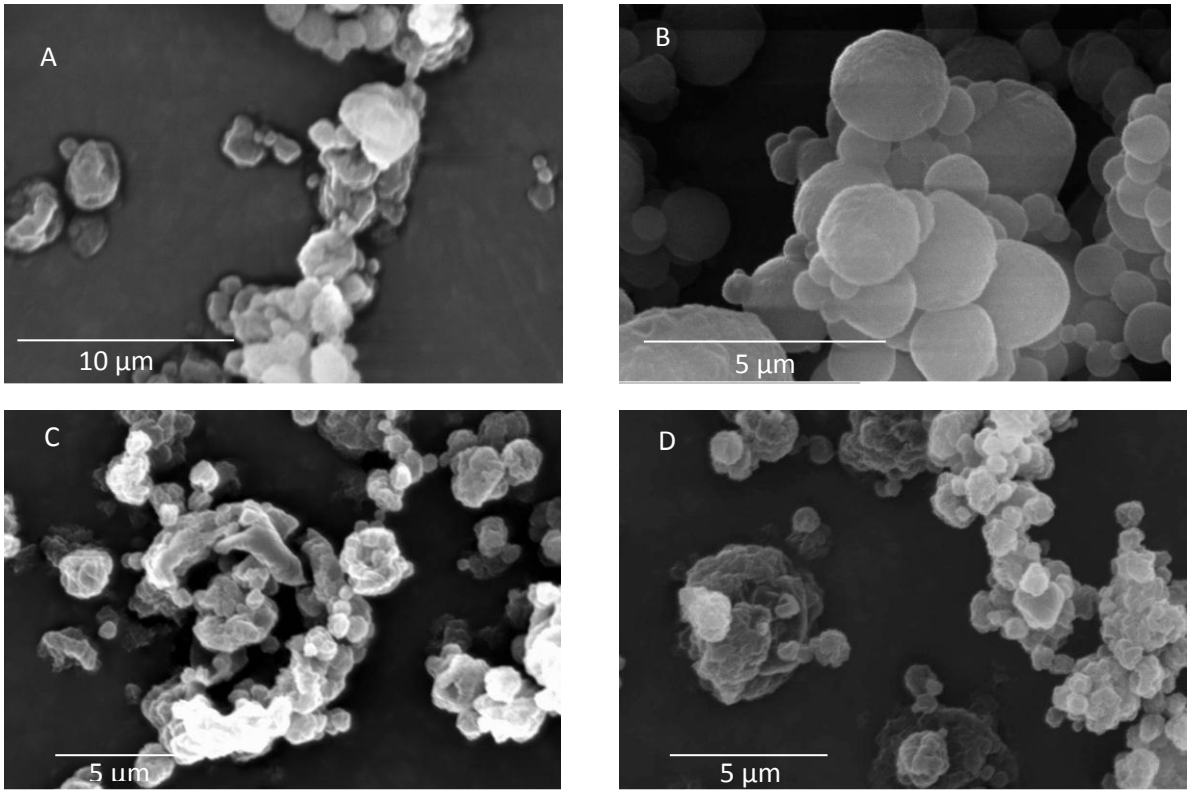

605 **Figure 2.** ***Scanning electron microscopy images of spray dried microparticles using Eudragit L100 with (A) 0% and (B)***
606 ***10%, hydrocortisone loading and AQOAT-AS-MG with (C) 0% and (D) 2.5% drug loading.***

607

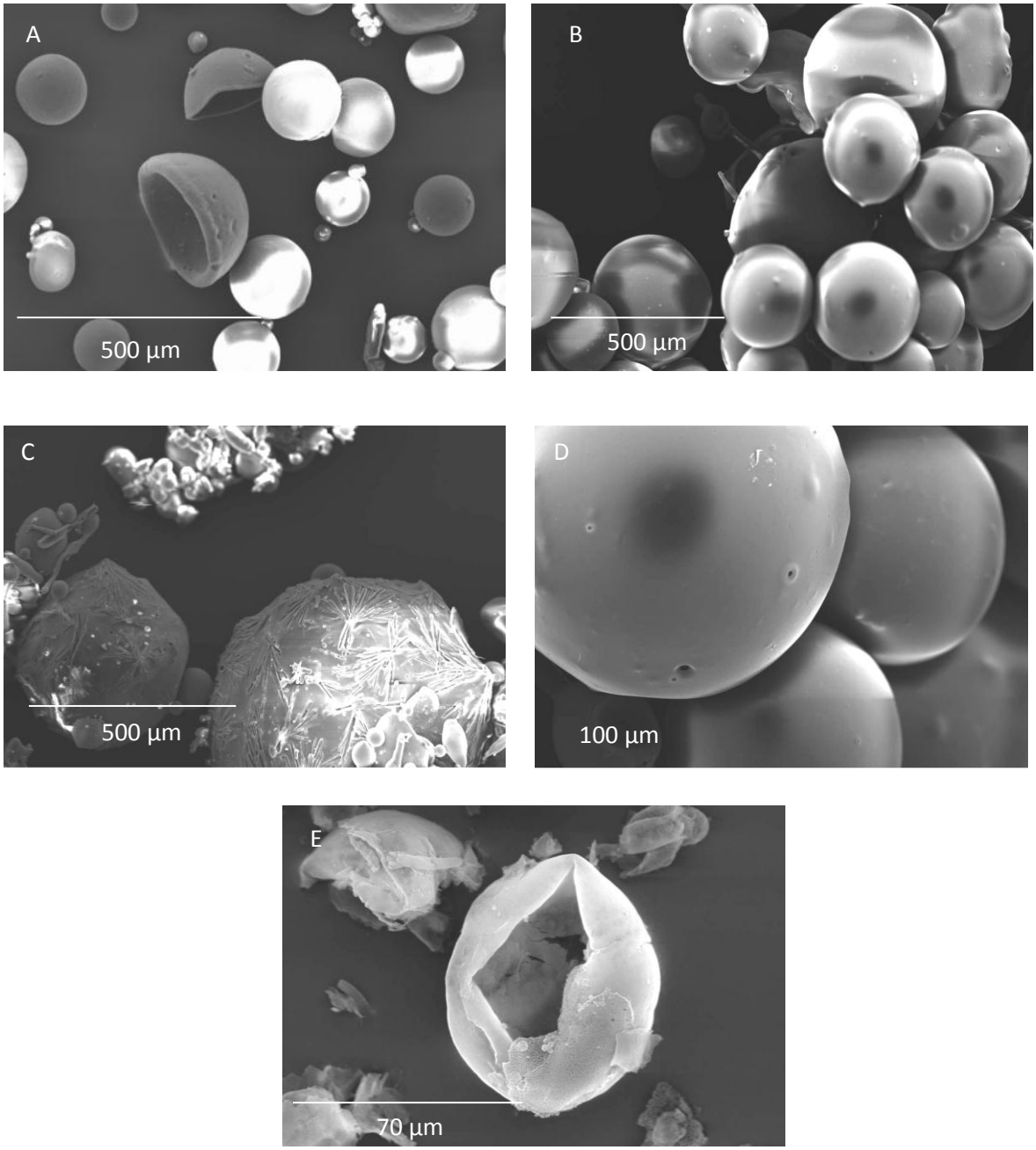

608 **Figure 3.** ***Scanning electron microphotographs of microparticles prepared by the oil in water emulsification solvent***
609 ***evaporation method; (A) , (B) and (C) show AQOAT AS-MG microparticles at 0%, 2.5% and 25% hydrocortisone loading***
610 ***respectively. Image D and E shows 2.5% w/w hydrocortisone-loaded AQOAT microparticles at high magnification and***
611 ***drug-free Eudragit L100 microparticles respectively.***

612

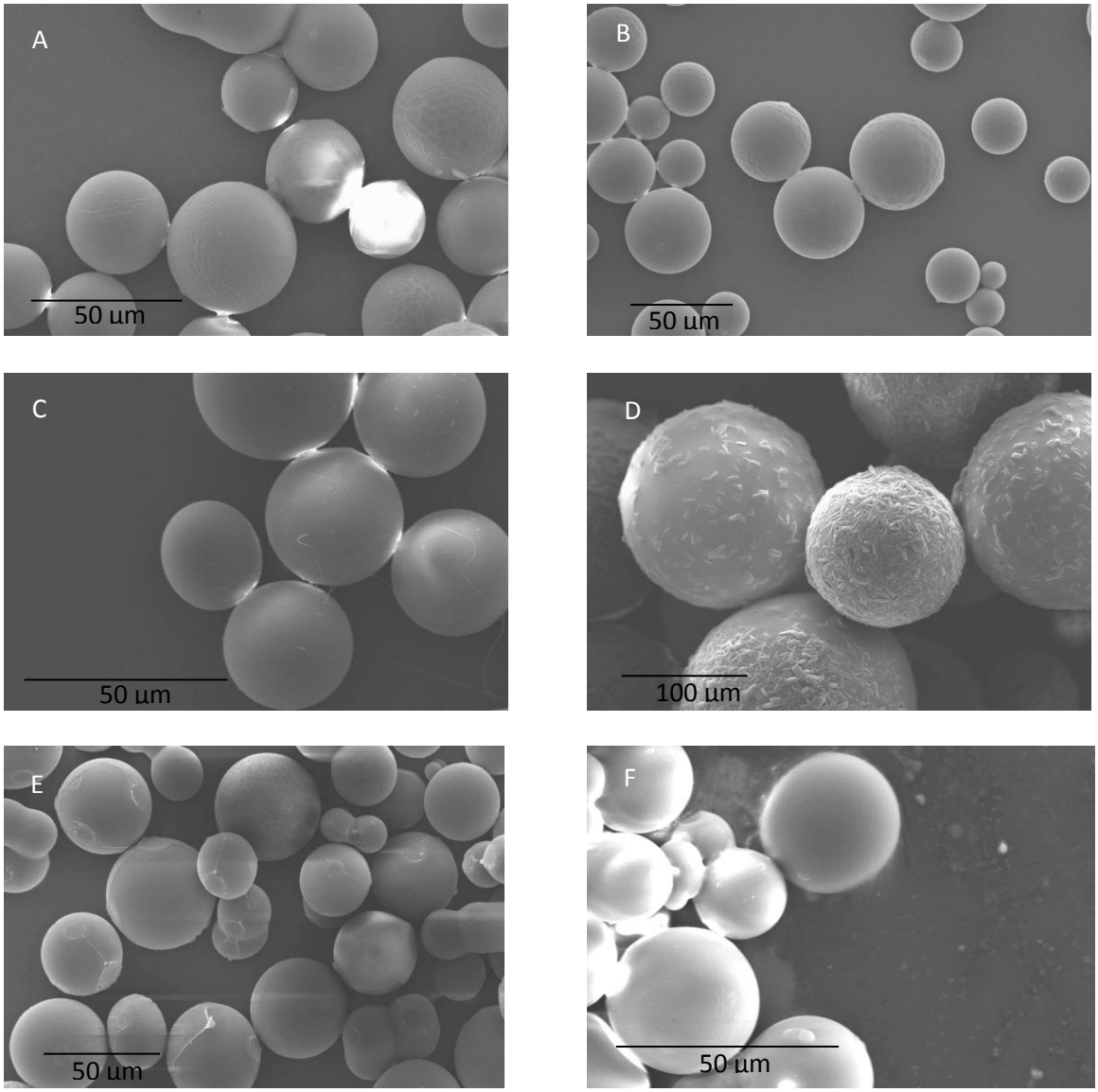

613 **Figure 4.** ***SEM photomicrographs of Eudragit L100 microparticles prepared from the oil-in-oil emulsification process at;***
614 ***(A) 0%, (B) 2.5%, (C) 10% and (D) 25% w/w theoretical hydrocortisone loading with respect to polymer. Images E and F***
615 ***show AQOAT AS-MG microparticles prepared at 0% and 2.5% hydrocortisone loading respectively.***

616

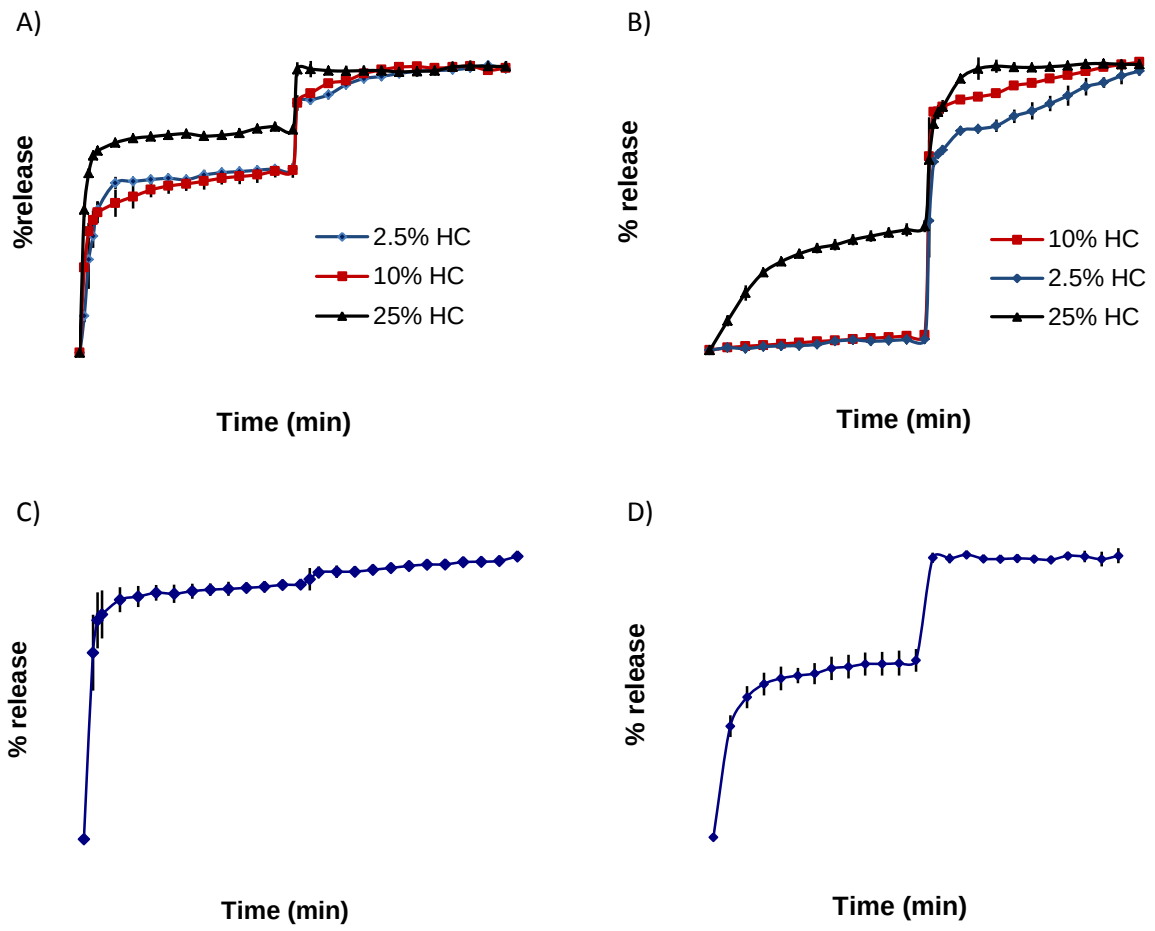

617 **Figure 5.** ***Stepped dissolution testing of prepared microparticles with pH change from 5 to 7 after 2 hrs; (A)spray dried***
618 ***Eudragit L100 microparticles at different hydrocortisone loadings, (B) Eudragit L100 microparticles prepared using the***
619 ***oil-in-oil microencapsulation method, (C) 2.5% hydrocortisone-loaded AQOAT AS-MG spray dried microparticles and (D)***
620 ***2.5% hydrocortisone-containing AQOAT AS-MG microparticles obtained from the oil-in-oil technique. HC denotes***
621 ***hydrocortisone. (mean±SD, n=3).***

622

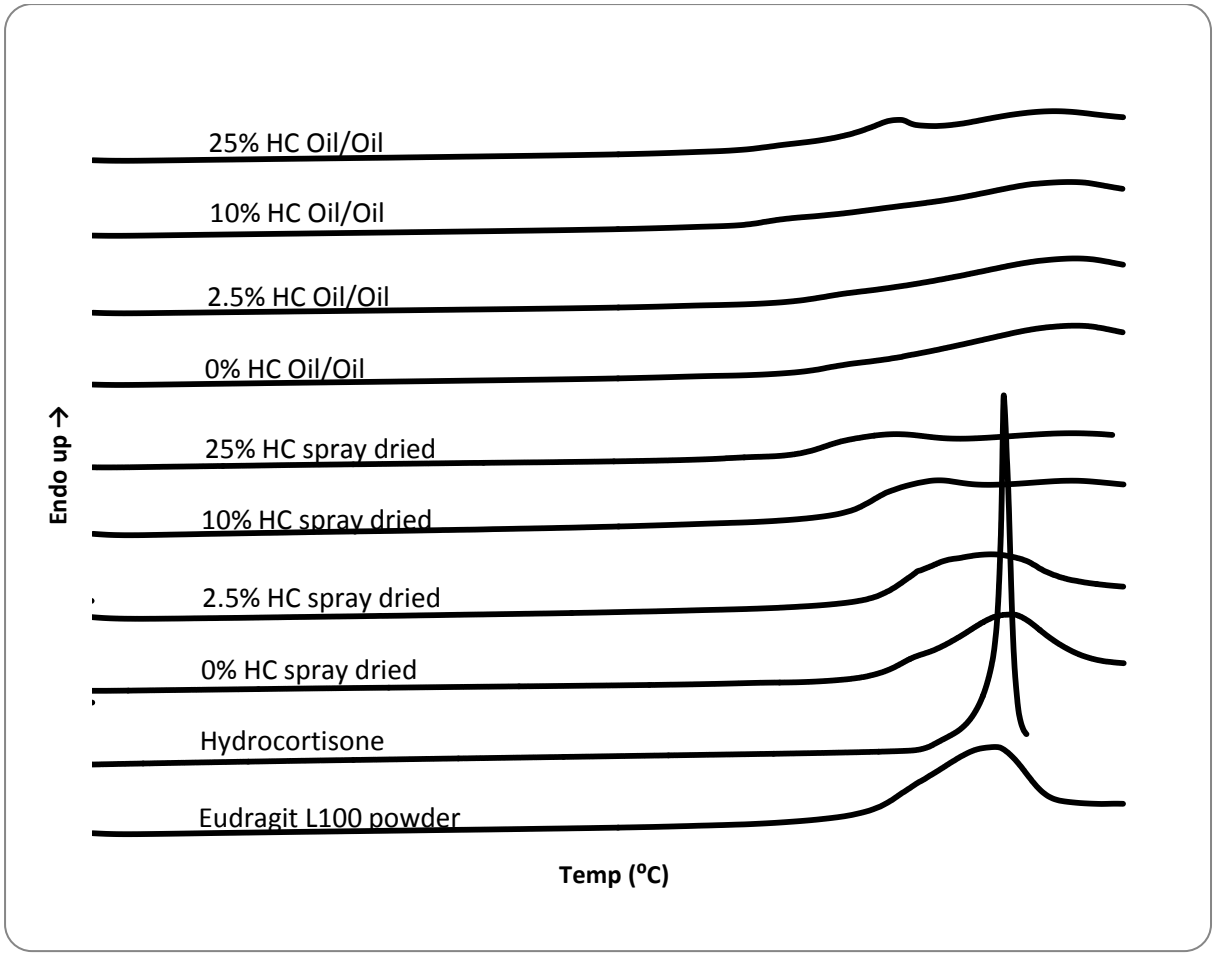

623

624 **Figure 6.** ***DSC thermograms of Eudragit L100 powder, hydrocortisone, drug-free and hydrocortisone-loaded Eudragit L100***
625 ***microparticles produced from the spray drying and the oil in oil microencapsulation method.***

626

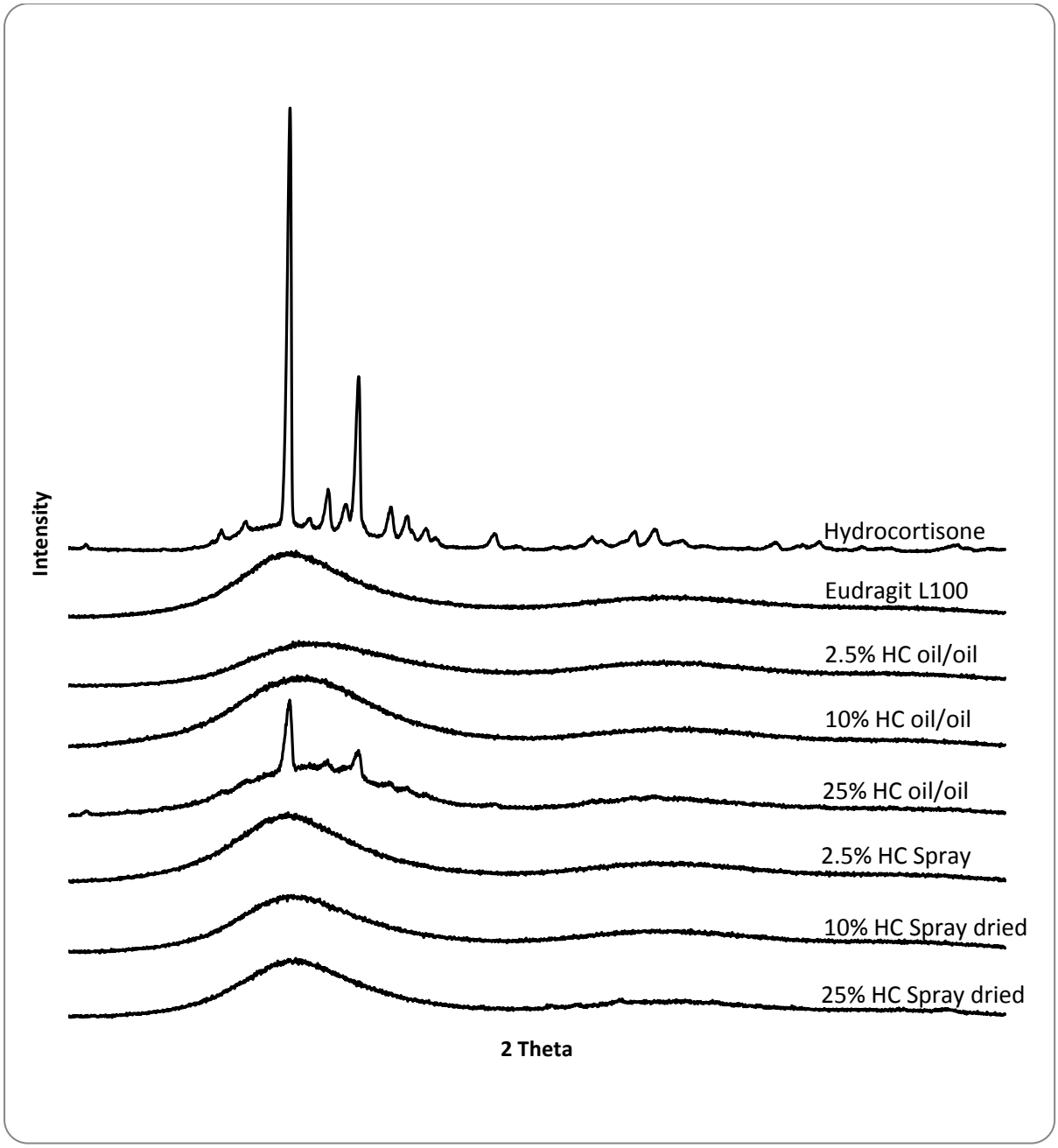

627

628 **Figure 7.** ***X-ray analysis of starting materials (hydrocortisone and Eudragit L100) and hydrocortisone-loaded***
629 ***microparticles prepared from the oil-in-oil encapsulation method and spray drying.***

630

631

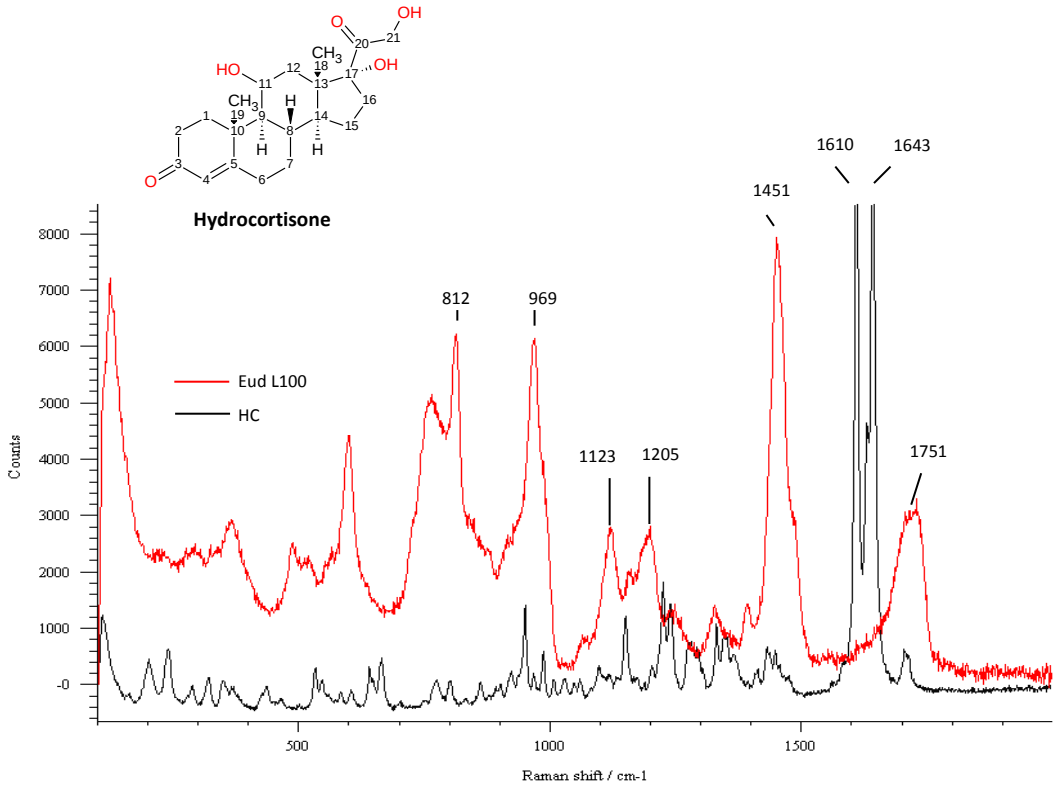

632

633 **Figure 8. Raman spectra of hydrocortisone (black line) and Eudragit L100 (red line).**

634

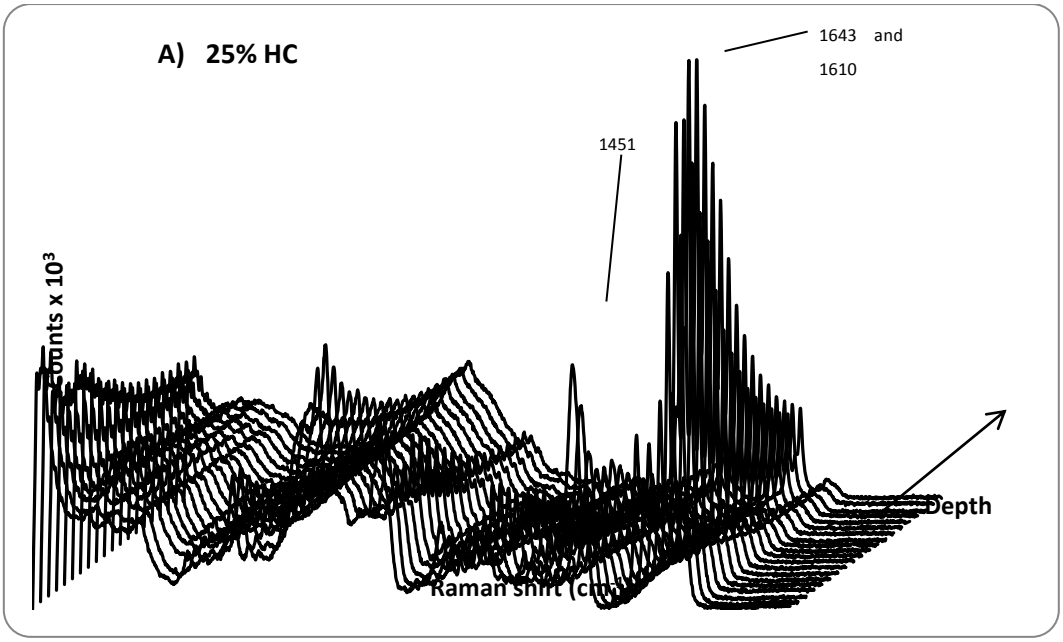

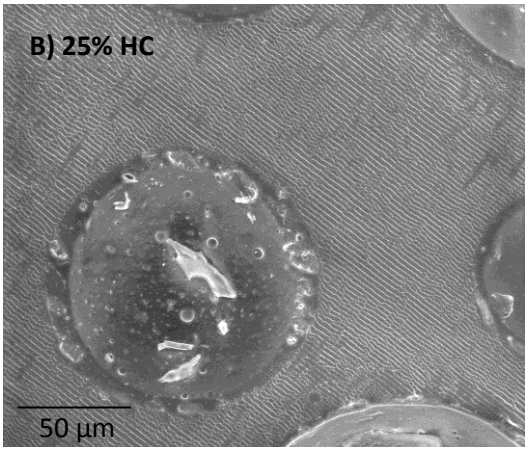

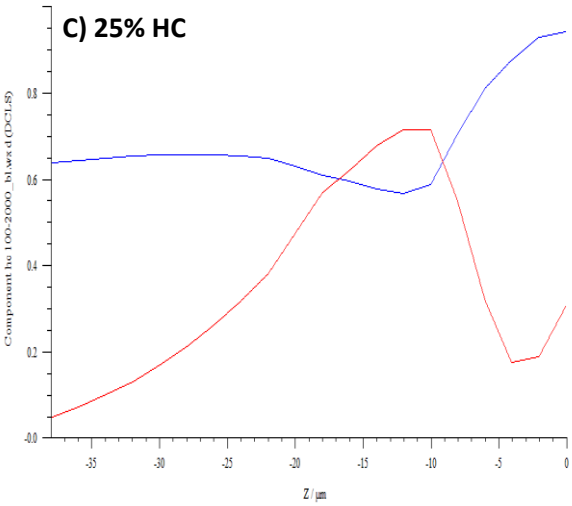

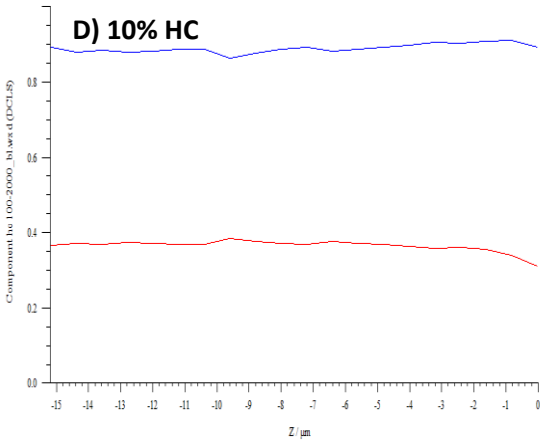

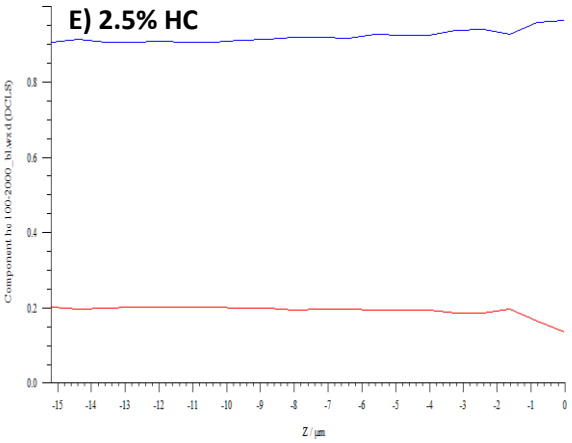

Figure 9. Raman depth profiling (A) and scanning electron microscopy (B) showing the internal composition of 25% w/w hydrocortisone-loaded microparticles prepared from the oil-in-oil microencapsulation technique. (C), (D) and (E) represents the *component analysis of hydrocortisone (red line) and Eudragit L100 (blue line) within the oil-in-oil prepared microparticles as a function of depth. Depth profiling was performed from the surface (0 µm) to a depth of -15.2 µm for 2.5% (E) and 10% w/w (D) hydrocortisone-loaded microparticles and -38.0 µm for 25% w/w drug-containing microparticles (C). HC denotes hydrocortisone.*

642 **Table 1.** ***Yield, tap density and encapsulation efficiency values of Eudragit L100 and AQOAT AS-MG microparticles***
643 ***prepared by spray drying with variable hydrocortisone loadings.***

Polymer	Drug loading (% w/w)	Yield (%)	Tap density (g/ml)	Encapsulation Efficiency (%)
Eudragit L100	0*	80.6	0.85±0.02	/
Eudragit L100	2.5*	78.7	0.84±0.04	99.1±2.99
Eudragit L100	10	47.7	0.92±0.03	88.6±3.63
Eudragit L100	25*	67.6	1.02±0.01	94.6±1.00
AQOAT AS-MG	0	53.1	0.57±0.03	/
AQOAT AS-MG	2.5	72.7	0.59±0.04	98.9±0.92

644 *Data from Rizi et al. (2010) shown for comparison.

645

Table 2. ***Yield and encapsulation efficiency of hydrocortisone-loaded AQOAT AS-MG microparticles prepared from the oil-in-water emulsification process.***

Drug loading (% w/w)	Yield (%)	Tap density (g/ml)	Encapsulation efficiency (%)
0	88.0	0.31±0.01	NA
2.5	63.2	0.25±0.02	23.35±1.09
25	77.1	0.15±0.01	22.05±1.02

649 **Table 3.** ***Yield, tap density and encapsulation efficiency values of Eudragit L100 and AQOAT AS-MG microparticles***
650 ***prepared from the oil-in-oil emulsification method at variable hydrocortisone loadings.***

Polymer	**Drug loading (% w/w)**	**Yield (%)**	**Tap density (g/ml)**	**Encapsulation Efficiency (%)**
Eudragit L100	0	81.3	0.86±0.05	/
Eudragit L100	2.5	89.5	1.03±0.01	94.84±1.79
Eudragit L100	10	90.7	1.02±0.07	82.04±0.74
Eudragit L100	25	86.0	0.33±0.02	73.62±2.38
AQOAT AS-MG	0	86.7	0.66±0.03	/
AQOAT AS-MG	2.5	90.7	0.86±0.04	100.9±2.9

651

652

653 **Table 4.** ***Residual solvent content (% w/w) of the microparticles (MPs) prepared from the oil-in-oil and spray drying***
654 ***methods.***

Hydrocortisone-loading	Spray dried MPs	Oil-in-oil MPs
0%	6.97±0.38	7.74±0.06
2.5%	7.33±1.08	7.64±0.10
10%	7.41±0.56	7.59±0.14
25%	6.59±0.79	7.80±0.38

655

5 References

[1]. Freitas S, Merkle HP, Gander B. Microencapsulation by solvent extraction/evaporation: reviewing the state of the art of microsphere preparation process technology. *J Controlled Release.* 2005;102(2):313-332.

[2]. Wischke C, Schwendeman SP. Principles of encapsulating hydrophobic drugs in PLA/PLGA microparticles. *Int J Pharm.* 2008;364(2):298-327.

[3]. Pinto Reis C, Neufeld RJ, Ribeiro AJ, Veiga F. Nanoencapsulation I. Methods for preparation of drug-loaded polymeric nanoparticles. *Nanomed Nanotechnol Biol Med.* 2006;2(1):8.

[4]. Fessi H, Puisieux F, Devissaguet JP. Nanocapsule formation by interfacial polymer deposition following solvent displacement. *Int J Pharm.* 1989;55:R1-R4.

[5]. Gao Y, Cui F, Guan Y, Yang L, wang Y, Zhang L. Preparation of roxithromycin-polymeric microspheres by the emulsion solvent diffusion method for taste masking. *Int J Pharm.* 2006;318:62-69.

[6]. Dong W, Bodmeier R. Encapsulation of lipophilic drugs within enteric microparticles by a novel coacervation method. *Int J Pharm.* 2006;326(1-2):128.

[7]. Bodmeier R, Chen H. Preparation of biodegradable poly(±)lactide microparticles using a spray-drying technique. *J Pharm Pharmacol.* 1988;40(11):754-757.

[8]. Palmieri G, Bonacucina G, Di Martino P, Martelli S. Spray-drying as a method for microparticulate controlled release systems preparation: Advantages and limits. I. Water-soluble drugs. *Drug Dev Ind Pharm.* 2001;27(3):195.

[9]. Hegazy N, Demirel M, Yazan Y. Preparation and in vitro evaluation of pyridostigmine bromide microparticles. *Int J Pharm.* 2002;242(1-2):171.

[10]. Xu J, Bovet LL, Zhao K. Taste masking microspheres for orally disintegrating tablets. *Int J Pharm.* 2008;359(1-2):63-69.

[11]. Wang F-J, Wang C-H. Sustained release of etanidazole from spray dried microspheres prepared by non-halogenated solvents. *J Controlled Release.* 2002;81:263-280

[12]. Makhlof A, Tozuka Y, Takeuchi H. pH-Sensitive nanospheres for colon-specific drug delivery in experimentally induced colitis rat model. *Eur J Pharm Biopharm.* 2009;72(1):1-8.

[13]. Bain DF, Munday DL, Smith A. Solvent influence on spray-dried biodegradable microspheres. *J Microencapsul.* 1999;16(4):453-474.

[14]. Vehring R. Pharmaceutical particle engineering via spray drying. *Pharm Res.* 2008;25(5):999-1022.

[15]. Bell SEJ, Dennis AC, Fido LA, et al. Characterization of silicone elastomer vaginal rings containing HIV microbicide TMC120 by Raman spectroscopy. *J Pharm Pharmacol.* 2007;59(2):203-207.

[16]. Giunchedi P, Alpar HO, Conte U. PDLLA microspheres containing steroids: spray drying, o/w and w/o/w emulsification as preparation methods. *J Microencapsul.* 1998;15:185-195.

[17]. Rizi K, Donaldson M, Green R, Williams A. Using pH abnormalities in diseased skin to trigger and target topical therapy. Pharm Res: Submitted.

[18]. Sparavigna A, Setaro M, Gualandri V. Cutaneous pH in children affected by atopic dermatitis and in healthy children: a multicenter study. Skin Res Technol. 1999;5(4):221-7.

[19]. Kendall RA, Alhnan MA, Nilkumhang S, Murdan S, Basit AW. Fabrication and in vivo evaluation of highly pH-responsive acrylic microparticles for targeted gastrointestinal delivery. *Eur J Pharm Sci.* 2009;37(3-4):284-290.

[20]. Healy AM, McDonald BF, Tajber L, Corrigan OI. Characterisation of excipient-free nanoporous microparticles (NPMPs) of bendroflumethiazide. *Eur J Pharm Biopharm.* 2008;69(3):1182-1186.

[21]. Sansone F, Aquino RP, Gaudio PD, Colombo P, Russo P. Physical characteristics and aerosol performance of naringin dry powders for pulmonary delivery prepared by spray-drying. *Eur J Pharm Biopharm.* 2009;72(1):206-213.

[22]. Florey K, ed. *Triamcinolone*. New York: Academic Press; 1977. Analytical profiles of drug substances; No. 1.

[23]. Ahmed A, Barry BW, Williams AC, Davis AF. Penciclovir solubility in Eudragit films: a comparison of X-ray, thermal, microscopic and release rate techniques. *J Pharm Biomed Anal.* 2004;34(5):945-956.

[24]. Rizi K, Green RJ, Donaldson M, Williams AC. Production of pH-responsive microparticles by spray drying: Investigation of experimental parameter effects on morphological and release properties. *J Pharm Sci.* 2010;100(2):566-579.

[25]. Friesen DT, Shanker R, Crew M, Smithey DT, Curatolo WJ, Nightingale JAS. Hydroxypropyl Methylcellulose Acetate Succinate-Based Spray-Dried Dispersions: An Overview. *Mol Pharmaceutics.* 2008;5(6):1003-1019.

[26]. Technical bulletin: Shin-Estu AQOAT: Shin-Estu Chemical Co.Ltd; 2006.

[27]. Wu P, Huang Y-B, Chang J-S, Tsai M-J, Tsai Y-H. Design and evaluation of sustained release microspheres of potassium chloride prepared by Eudragit®. *Eur J Pharm Sci.* 2003;19:115-122.

[28]. Pignatello R, Bucolo C, Ferrara P, Maltese A, Puleo A, Puglisi G. Eudragit RS100 nanosuspensions for the ophtalmic controlled delivery of ibuprofen. *Eur J Pharm Sci.* 2002;16:53-61.

[29]. Meissner Y, Pellequer Y, Lamprecht A. Nanoparticles in inflammatory bowel disease: particles targeting versus pH-sensitive delivery. *Int J Pharm.* 2006;316:138-143.

[30]. Lamprecht A, Yamamoto H, Takeuchi H, Kawashima Y. Design of pH-sensitive microspheres for the colonic delivery of the immunosuppressive drug tacrolimus. *Eur J Pharm Biopharm.* 2004;58(1):37-43.

[31]. Lamprecht A, Yamamoto H, Takeutchi H, Kawashima Y. pH-sensitive microsphere delivery increases oral bioavailability of calcitonin. *J Controlled Release.* 2004;98:1-9.

[32]. Rowe RC, Sheskey PJ, Owen SC, (ed). *Handbook of pharmaceutical excipients*. 5th ed: Pharmaceutical Press; 2006.

[33]. Yang M, Cui F, You B, et al. A novel pH-dependent gradient-release delivery system for nitrendipine: I. Manufacturing, evaluation in vitro and bioavailability in healthy dogs. *J Controlled Release.* 2004;98(2):219-229.

[34]. You J, Cui F-d, Li Q-p, Han X, Yu Y-w, Yang M-s. A novel formulation design about water-insoluble oily drug: preparation of zedoary turmeric oil microspheres with self-emulsifying ability and evaluation in rabbits. *Int J Pharm.* 2005;288(2):315-323.

[35]. Sato Y, Kawashima Y, Takeutchi H, Yamamoto H. Physicochemical properties to determine the buoyancy of hollow microparticles (microballons) prepared by the emulsion solvent diffusion method. *Eur J Pharm Biopharm.* 2003;55:297-304.

[36]. Augsburger LL, Hoag SW. *Pharmaceutical Dosage Forms: Unit operations and mechanical properties.* Vol 1. 3rd ed: Informa Health Care; 2008.

[37] Siepmann J, Faisant N, Akiki J, Richard J, Benoit P. Effect of the size of biodegradable microparticles on drug release: experiment and theory. *J Controlled Release. 2004; 96(1): 123-134.*

[38]. Kim EH-J, Chen XD, Pearce D. On the mechanisms of surface formation and the surface compositions of industrial milk powders. *Drying Technol.* 2003;21(2):265 - 278.

[39]. Nilkumhang S, Alhnan MA, McConnell EL, Basit AW. Drug distribution in enteric microparticles. *Int J Pharm.* 2009;379(1):1-8.

[40]. Vanber R. Formation and physical characterisation of large porous particles for inhalation. *Pharm Res.* 1999;16(11):1735-1742.

[41]. Nilkumhang S, Basit AW. The robustness and flexibility of an emulsion solvent evaporation method to prepare pH-responsive microparticles. *Int J Pharm.* 2009;377(1-2):135-141.

[42]. Yadav A, Yadav V. Preparation and evaluation of polymeric carbamazepine spherical crystals by emulsion solvent diffusion technique*. Asia J Pharm.* 2009; 3: 18-25.

[43]. Dubernet C. Thermoanalysis of microspheres. *Thermochim Acta.* 1995;248:259.
[44]. Lin S-Y, Liao C-M, Husiue G-H, Liang R-C. Study of a theophylline-Eudragit L mixture using a combined system of microscopic Fourier-transform infrared spectroscopy and differential scanning calorimetry. *Thermochimica Acta.* 1995;245(153-166).
[45]. Velaga SP, Ghaderi R, Carlfors J. Preparation and characterisation of hydrocortisone particles using a supercritical fluids extraction process. *Int J Pharm.* 2002;231(2):155-166.
[46]. Fleming OS, Chan KLA, Kazarian SG. FT-IR imaging and Raman microscopic study of poly(ethylene terephthalate) film processed with supercritical CO2. *Vil Spectrosc.* 2004;35(1-2):3-7.
[47]. Salmain M, Vessières A, Top S, Jaouen G, Butler IS. Analytical potential of near-infrared fourier transform Raman spectra in the detection of solid transition metal carbonyl steroid hormones. *J Raman Spectrosc.* 1995;26(1):31-38.
[48]. Socrates G. *Infrared and Raman characteristic group frequencies: tables and charts*. 3rd ed. Chichester: John Wiley & Sons; 2001.
[49]. Pelletier MJ, ed. *Analytical applications of Raman spectroscopy.* 1st ed. Oxford: Blackwell Science; 1999.